# Supplementary Information

# Charge Assisted Non-volatile Magnetoelectric Effects in $NiFe_2O_4$/PMN-PT Heterostructures

Xin Pang, Chao Jin,* Guoqin Gao, Dong Li, Dongxing Zheng, and Haili Bai*

*Tianjin Key Laboratory of Low Dimensional Materials Physics and Processing Technology, Faculty of Science, Tianjin University, Tianjin 300350, P.R. China*

*E–mail: chaojin@tju.edu.cn

*E–mail: baihaili@tju.edu.cn

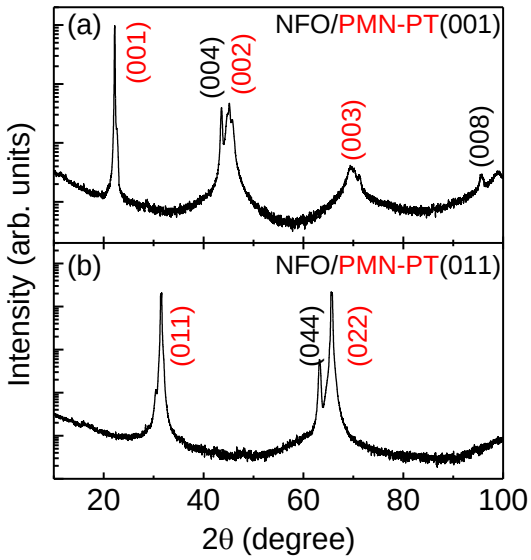


**Fig. S1.** XRD patterns of the (a) (001)-oriented and (b) (011)-oriented NFO (50 nm)/PMN-PT heterostructures.

Figure S1 shows the XRD patterns of the NFO (50 nm)/PMN-PT heterostructures. The out-of-plane lattice parameters of (001) and (011) NFO film are ~8.30±0.10 and ~8.31±0.07 Å, respectively.

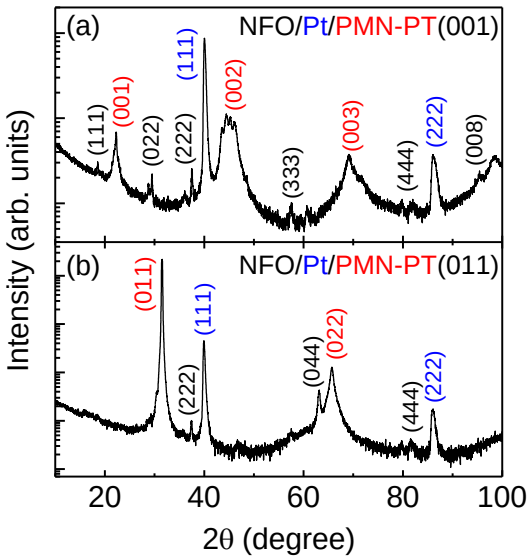


**Fig. S2.** XRD patterns of the (a) (001)-oriented and (b) (011)-oriented NFO/Pt/PMN-PT heterostructures. The thicknesses of NFO and Pt are 100 nm and 10 nm, respectively.

Figure S2 presents the XRD patterns of NFO (100 nm)/Pt/PMN-PT heterostructures. The (111) and (222) diffraction peaks of the Pt buffer layer are observed. The NFO films deposited on the Pt buffer layers are polycrystalline. For the NFO film in the (011) heterostructure, the (222), (444) and (044) peaks are shown in the Fig. S2b.

Figure S3 shows the AFM images of the NFO (100 nm)/PMN-PT and NFO (100 nm)/Pt/PMN-PT heterostructures. The films have smooth surface in the NFO/PMN-PT heterostructures. The average roughnesses ($R_a$) of the films are about 0.76 and 1.68 nm in (001) and (011) NFO/PMN-PT heterostructures, 19.20 and 6.53 nm in (001) and (011) NFO/Pt/PMN-PT heterostructures, respectively. The AFM scan lines across the surfaces of the NFO series heterostructures are displayed in the Fig. S4.

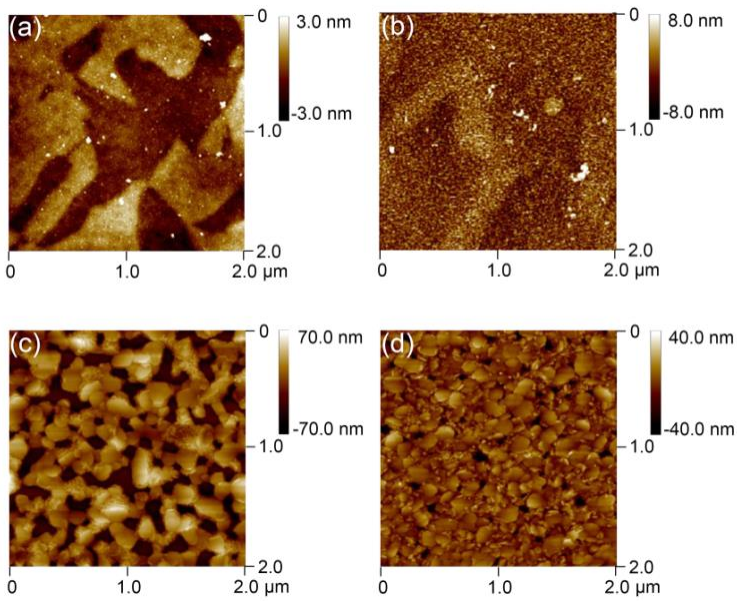


**Fig. S3.** (a), (b) AFM images of the (001) and (011) NFO (100 nm)/PMN-PT heterostructures, respectively. (c), (d) AFM images of the (001) and (011) NFO (100 nm)/Pt (10 nm)/PMN-PT heterostructures, respectively.

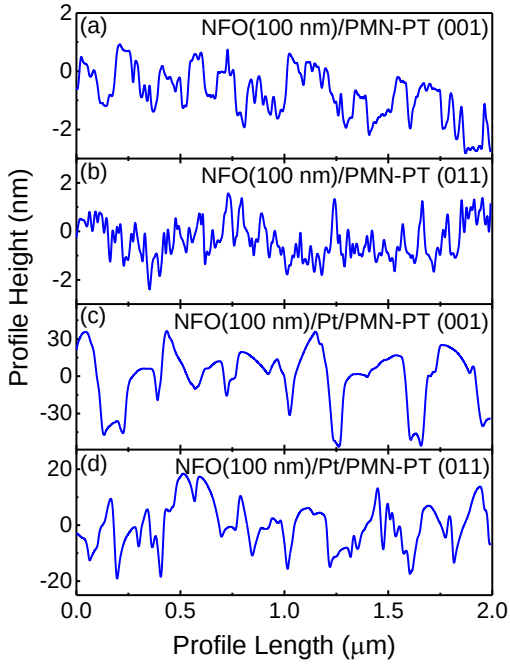


**Fig. S4.** (a), (b) AFM scan lines across the surface of the (001) and (011) NFO/PMN-PT heterostructures, respectively. (c), (d) AFM scan lines across the surface of the (001) and (011) NFO/Pt/PMN-PT heterostructures, respectively.

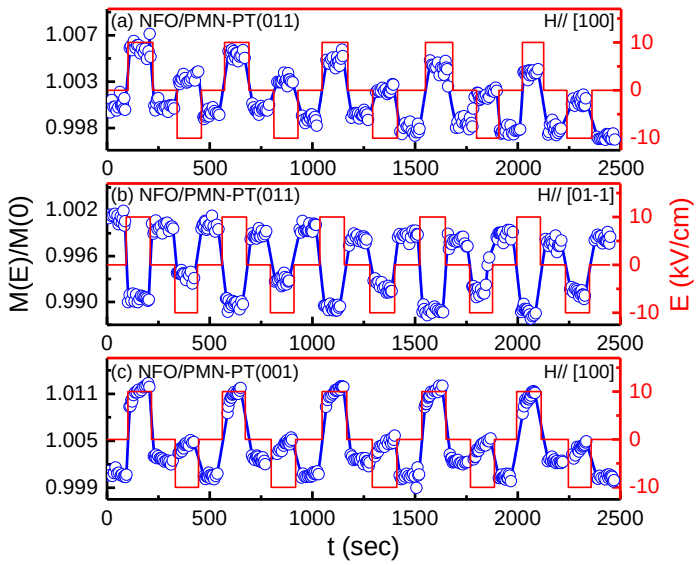


**Fig. S5.** Time-dependent $M(E)/M(0)$ curves of the (011) NFO (50 nm)/PMN-PT heterostructures with the magnetic field of 2.0 kOe along (a) [100] and (b) [01-1] directions, respectively. (c) Time-dependent $M(E)/M(0)$ curves of (001) NFO (50 nm)/PMN-PT with 3.0 kOe magnetic field along the [100] direction.

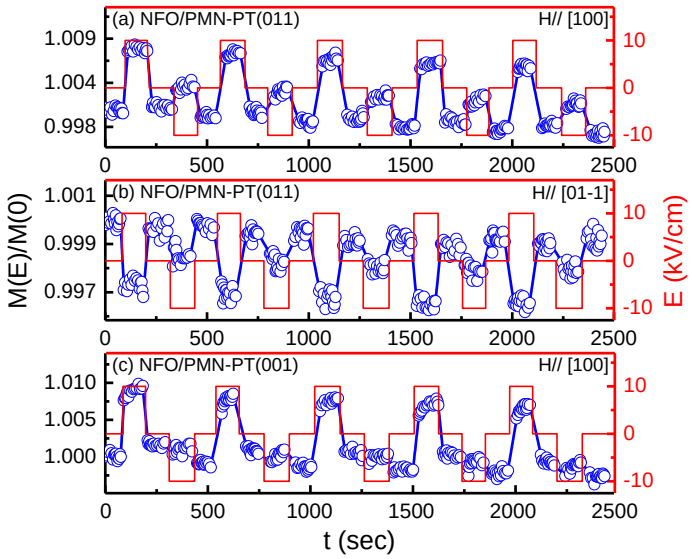


**Fig. S6.** Time-dependent $M(E)/M(0)$ curves of the (011) NFO (225 nm)/PMN-PT heterostructures with the magnetic field of 4.0 kOe along (a) [100] and (b) [01-1] directions, respectively. (c) Time-dependent $M(E)/M(0)$ curves of (001) NFO (225 nm)/PMN-PT with 4.0 kOe magnetic field along the [100] direction.

**Tab. S1.** $H_C$ and $M_R$ in five states measured along the [100] direction of the NFO/PMN-PT (011) and NFO/Pt/PMN-PT (011) heterostructures.

| $E$ (kV/cm) | 0 | +10 | +0 | –10 | –0 |
|---|---|---|---|---|---|
| $M_R$ (emu/cm$^3$) | 52.11 | 54.02 | 52.49 | 53.47 | 52.30 |
| $H_C$ (Oe) | 572 | 585 | 571 | 583 | 572 |
| $M_{R,Pt}$ (emu/cm$^3$) | 33.08 | 39.16 | 34.15 | 34.79 | 33.03 |
| $H_{C,Pt}$ (Oe) | 371 | 440 | 378 | 390 | 371 |

Figure S5 shows the $M(E)/M(0)$ versus time curves at different electric fields. The magnetization along the in-plane [100] direction in the 50-nm-thick NFO film

increases when applying the out-of-plane electric fields. When applying the in-plane magnetic field along the [01-1] direction in the (011) NFO/PMN-PT heterostructure, the magnetization decreases. And it is clear that the magnetization variation is asymmetric under the positive and negative fields, suggesting that another effect should be considered. The oxygen vacancies migration under the electric fields can cause the asymmetric magnetization variation. At the same time, we measured other heterostructures with the NFO thickness of 225 nm. Similar magnetic transformations were detected, as illustrated in Fig. S6. The $M_R$ and $H_C$ of the NFO (100 nm)/PMN-PT (011) and the NFO (100 nm)/Pt/PMN-PT (011) along the [100] direction were displayed in the Tab. S1. The changes of $M_R$ and $H_C$ perform the similar trend as the magnetization versus electric field.

The existence of oxygen vacancies of the NFO film were characterized by XPS. The XPS spectra of Fe 2*p*, Ni 2*p* and O 1*s* are displayed in Fig. S7. The Ni/Fe ratio is measured of 1:2. The presence of $Fe^{2+}$ in the NFO film indicates the existence of oxygen vacancies. In the O 1*s* XPS spectrum, the broadened peak of O 1*s* can be fitted with two components: the first peak around 530.0 eV is assigned to $O^{2-}$, and the second peak located at 531.5 eV is assigned to $O^{-}$ or $O_2^{2-}$, which could be attributed to the intrinsic oxygen vacancy on the surface.

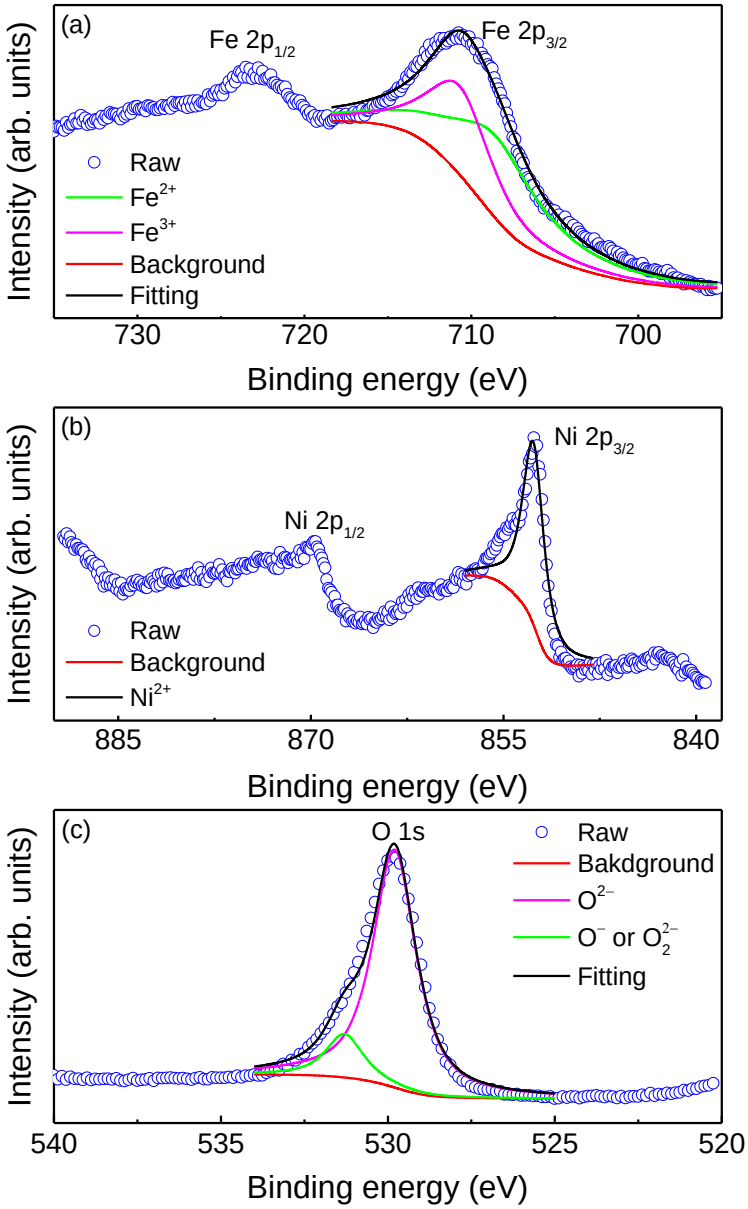


**Fig. S7.** XPS spectra of the NFO (100 nm)/PMN-PT (011) heterostructure in the region of (a) Fe 2*p*, (b) Ni 2*p* and (c) O 1*s* peaks.

The imparities in magnetization $\Delta M$ between the positive and negative electric fields in the NFO/PMN-PT heterostructures gradually diminish along the [01-1] direction, as shown in Fig. S8. The values in 50, 100, and 225 nm films are ~0.20, ~0.16 and ~0.03 emu/cm$^3$, respectively.

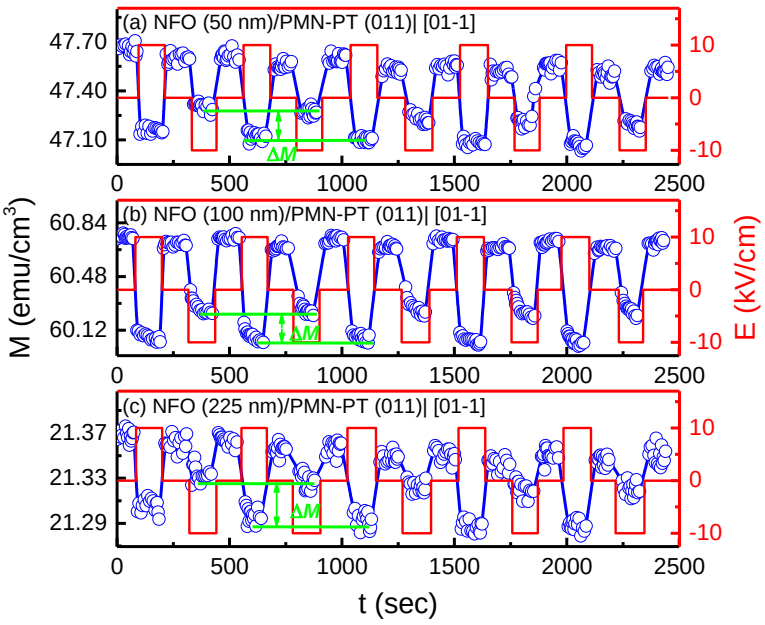


**Fig. S8.** *M*(*E*)–*t* of the NFO/PMN-PT (011) heterostructures measured along the [01-1] direction at 300 K with different NFO thicknesses. The thickness of NFO films are (a) 50, (b) 100 and (c) 225 nm.